

# Neutrino and antineutrino cross sections in $^{12}\text{C}$

A. R. Samana<sup>1</sup>, F. Krmpotić<sup>2</sup>, N. Paar<sup>3</sup>, and C. A. Bertulani<sup>4</sup>

<sup>1</sup> Departamento de Cs. Exactas e Tecnológicas, UESC, Brasil

<sup>2</sup> Instituto de Física La Plata, Universidad Nacional de La Plata, La Plata, Argentina

<sup>3</sup> Physics Department, Faculty of Science, University of Zagreb, Croatia

<sup>4</sup> Department of Physics, Texas A&M University-Commerce, TX-USA

E-mail: krmpotic@fisica.unlp.edu.ar

**Abstract.** We extend the formalism of weak interaction processes, obtaining new expressions for the transition rates, which greatly facilitate numerical calculations, both for neutrino-nucleus reactions and muon capture. We have done a thorough study of exclusive (ground state) properties of  $^{12}\text{B}$  and  $^{12}\text{N}$  within the projected quasiparticle random phase approximation (PQRPA). Good agreement with experimental data is achieved in this way. The inclusive neutrino/antineutrino ( $\nu/\bar{\nu}$ ) reactions  $^{12}\text{C}(\nu, e^-)^{12}\text{N}$  and  $^{12}\text{C}(\bar{\nu}, e^+)^{12}\text{B}$  are calculated within both the PQRPA, and the relativistic QRPA (RQRPA). It is found that the magnitudes of the resulting cross-sections: i) are close to the sum-rule limit at low energy, but significantly smaller than this limit at high energies both for  $\nu$  and  $\bar{\nu}$ , ii) they steadily increase when the size of the configuration space is augmented, and particularly for  $\nu/\bar{\nu}$  energies  $> 200$  MeV, and iii) converge for sufficiently large configuration space and final state spin.

## 1. Introduction

The neutrino-nucleus scattering on  $^{12}\text{C}$  is important because this nucleus is a component of many liquid scintillator detectors. As such it has been employed in experimental facilities LSND, KARMEN, and LAMPF to search for neutrino oscillations, and for measuring neutrino-nucleus cross sections. The  $^{12}\text{C}$  target will be used as well in several planned experiments, such as the spallation neutron source (SNS) at Oak Ridge National Laboratory, and the Large Volume Detector (LVD) at Gran Sasso National Laboratories. On the other hand, this nucleus is important for astrophysics studies, as it forms one of the onion-like shells of large stars before they collapse. Concomitantly, the LVD group have stressed recently the importance of measuring supernova neutrino oscillations. A comprehensive theoretical review on neutrino-nucleus interaction was done by Kolbe *et al.* [1].

## 2. Formalism for the Weak Interacting Processes

The most widely used formalism for neutrino-nucleus scattering was developed by the Walecka group [2]. They classify the nuclear transition moments as Coulomb, longitudinal, transverse electric, and transverse magnetic. This terminology is not used in nuclear  $\beta$ -decay and  $\mu$ -capture, where one only speaks on vector and axial matrix elements with different degrees of forbiddenness: allowed (GT and Fermi), first forbidden, second forbidden, *etc.* Motivated by this fact, we extend the formalism of weak interaction processes developed in [3, 4], obtaining new expressions for the transition rates, which greatly facilitate numerical calculations, both for neutrino-nucleus reactions and muon capture.

The weak Hamiltonian is expressed in the form [2]

$$H_W(\mathbf{r}) = \frac{G}{\sqrt{2}} J_\alpha l_\alpha e^{-i\mathbf{r}\cdot\mathbf{k}}, \quad (1)$$

where  $G = (3.04545 \pm 0.00006) \times 10^{-12}$  is the Fermi coupling constant (in natural units), the leptonic current  $l_\alpha \equiv \{\mathbf{l}, il_\emptyset\}$  is given by [4, Eq. (2.3)] and the hadronic current operator  $J_\alpha \equiv \{\mathbf{J}, iJ_\emptyset\}$  in its nonrelativistic form [4]. The quantity  $k = P_i - P_f \equiv \{\mathbf{k}, ik_\emptyset\}$  is the momentum transfer,  $M$  is the nucleon mass, and  $P_i$  and  $P_f$  are momenta of the initial and final nucleon (nucleus). The effective vector, axial-vector, weak-magnetism and pseudoscalar dimensionless coupling constants are defined in [4]. In performing the multipole expansion of the nuclear operators  $O_\alpha \equiv (\mathbf{O}, iO_\emptyset) = J_\alpha e^{-i\mathbf{k}\cdot\mathbf{r}}$  it is convenient: 1) to take  $\mathbf{k}$  along the  $z$  axis, *i.e.*,  $e^{-i\mathbf{k}\cdot\mathbf{r}} \rightarrow e^{-ikz}$ , and 2) to make use of Racah's algebra. One obtains

$$O_{\emptyset J} = g_V \mathcal{M}_J^V + ig_A \mathcal{M}_J^A + i(\bar{g}_A + \bar{g}_{P1}) \mathcal{M}_{0J}^A \quad (2)$$

$$O_{mJ} = i(\delta_{m0} \bar{g}_{P2} - g_A + m\bar{g}_W) \mathcal{M}_{mJ}^A + g_V \mathcal{M}_{mJ}^V - \delta_{m0} \bar{g}_V \mathcal{M}_J^V, \quad (3)$$

with the elementary operators

$$\begin{aligned} \mathcal{M}_J^V &= j_J(\rho) Y_J(\hat{\mathbf{r}}), & \mathcal{M}_{mJ}^A &= \sum_{L \geq 0} i^{J-L-1} F_{LJm} j_L(\rho) [Y_L(\hat{\mathbf{r}}) \otimes \boldsymbol{\sigma}]_J, \\ \mathcal{M}_J^A &= M^{-1} j_J(\rho) Y_J(\hat{\mathbf{r}}) (\boldsymbol{\sigma} \cdot \boldsymbol{\nabla}), & \mathcal{M}_{mJ}^V &= M^{-1} \sum_{L \geq 0} i^{J-L-1} F_{LJm} j_L(\rho) [Y_L(\hat{\mathbf{r}}) \otimes \boldsymbol{\nabla}]_J, \end{aligned} \quad (4)$$

where  $F_{LJm}$  are Clebsch-Gordan coefficients [4]. The CVC relates the vector-current pieces of the operator  $O_\alpha$  as  $\mathbf{k} \cdot \mathbf{O}^V \equiv \kappa O_0^V = \tilde{k}_\emptyset O_\emptyset^V$  with  $\tilde{k}_\emptyset \equiv k_\emptyset - S(\Delta E_{\text{Coul}} - \Delta M)$ , where  $\Delta E_{\text{Coul}} \cong \frac{6e^2 Z}{5R} \cong 1.45ZA^{-1/3}$  MeV, is the Coulomb energy difference between the initial and final nuclei,  $\Delta M = M_n - M_p = 1.29$  MeV is the neutron-proton mass difference, and  $S = \pm 1$  for neutrino and antineutrino scattering, respectively.

The transition amplitude  $\mathcal{T}_{J_n^\pi}(\kappa) \equiv \sum_{s_\ell, s_\nu} |\langle J_n^\pi | H_W(\kappa) | 0^+ \rangle|^2$  for the neutrino-nucleus reaction at a fixed value of  $\kappa$ , from the initial state  $|0^+\rangle$  in the  $(Z, N)$  nucleus to the  $n$ -th final state  $|J_n^\pi\rangle$  in the nucleus  $(Z \pm 1, N \mp 1)$ , reads

$$\mathcal{T}_{J_n^\pi}(\kappa) = 4\pi G^2 \left[ \sum_{\alpha=\emptyset,0,\pm 1} |\langle J_n^\pi | O_{\alpha J}(\kappa) | 0^+ \rangle|^2 \mathcal{L}_\alpha - 2\Re(\langle J_n^\pi | O_{\emptyset J}(\kappa) | 0^+ \rangle \langle J_n^\pi | O_{0J}(\kappa) | 0^+ \rangle^*) \mathcal{L}_{\emptyset 0} \right], \quad (5)$$

where the momentum transfer is  $k = p_\ell - q_\nu$ , with  $p_\ell \equiv \{\mathbf{p}_\ell, iE_\ell\}$  and  $q_\nu \equiv \{\mathbf{q}_\nu, iE_\nu\}$ . The lepton traces  $\mathcal{L}_\emptyset, \mathcal{L}_0, \mathcal{L}_{\pm 1}$  and  $\mathcal{L}_{\emptyset 0}$  are defined in [4].

### 3. Neutrino (antineutrino)-nucleus cross section

The exclusive cross-section (ECS) for the state  $|J_n^\pi\rangle$ , as a function of the incident neutrino energy  $E_\nu$ , is

$$\sigma_\ell(J_n^\pi, E_\nu) = \frac{|\mathbf{p}_\ell| E_\ell}{2\pi} F(Z + S, E_\ell) \int_{-1}^1 d(\cos \theta) \mathcal{T}_{J_n^\pi}(\kappa), \quad (6)$$

where  $E_\ell = E_\nu - \omega_{J_n^\pi}$  and  $|\mathbf{p}_\ell|$  are the energy and modulus of linear momentum of the lepton  $\ell = e, \mu$ , and  $\omega_{J_n^\pi} = -k_\emptyset = E_\nu - E_\ell$  is the excitation energy of the state  $|J_n^\pi\rangle$  relative to the

state  $|0^+\rangle$ . Moreover,  $F(Z + S, E_\ell)$  is the Fermi function for neutrino ( $S = 1$ ), and antineutrino ( $S = -1$ ) processes, respectively. Here, we will also deal with the inclusive cross-sections (ICS),

$$\sigma_\ell(E_\nu) = \sum_{J_n^\pi} \sigma_\ell(J_n^\pi, E_\nu), \quad (7)$$

as well as with folded cross-sections, both exclusive, and inclusive

$$\bar{\sigma}_\ell(J_n^\pi) = \int dE_\nu \sigma_\ell(J_n^\pi, E_\nu) n_\ell(E_\nu) \quad , \quad \bar{\sigma}_\ell = \int dE_\nu \sigma_\ell(E_\nu) n_\ell(E_\nu), \quad (8)$$

where  $n_\ell(E_\nu)$  is the neutrino (antineutrino) normalized flux. In the evaluation of both neutrino, and antineutrino ICS the summation in (7) goes over all  $n$  states with spin and parity  $J^\pi \leq 7^\pm$  in the PQRPA (Projected Quasiparticle Random Phase Approximation), and over  $J^\pi \leq 14^\pm$  in the RQRPA (Relativistic QRPA).

#### 4. Numerical results

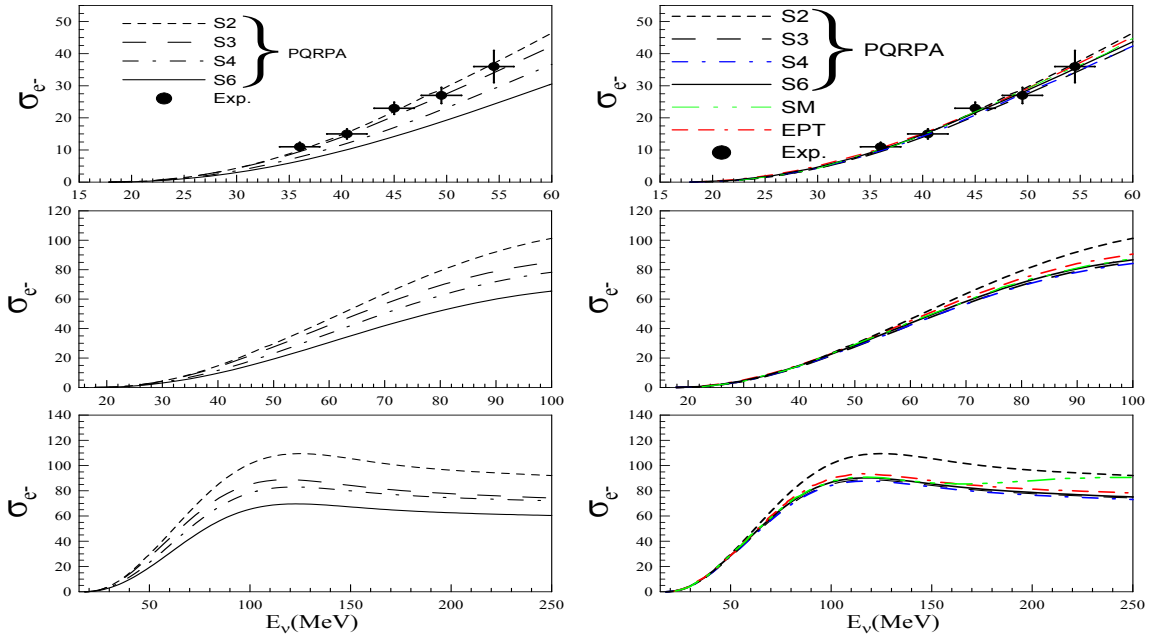


**Figure 1.** (Color online) ECS  $\sigma_{e^-}(1_1^+, E_\nu)$  for the reaction  $^{12}\text{C}(\nu_e, e^-)^{12}\text{N}$  (in units of  $10^{-42} \text{ cm}^2$ ), as a function of the incident neutrino energy  $E_\nu$ . On the left side we have  $t = 0$  for all  $S_N$ , whereas for the right side  $t = 0$  for  $S_2$ , and  $S_3$ ,  $t = 0.2$  for  $S_4$ , and  $t = 0.3$  for  $S_6$ . The experimental data in the DAR region are from Ref. [6].

The calculations were performed with the PQRPA using the model spaces  $S_2, S_3, S_4$ , and  $S_6$  including 2, 3, 4, and 6  $\hbar\omega$  harmonic oscillators shells, respectively, and by employing a  $\delta$ -interaction. For  $S_2, S_3$ , and  $S_4$  spaces the s.p. energies and pairing strengths were varied in a  $\chi^2$  search to account for the experimental spectra of odd-mass nuclei  $^{11}\text{C}$ ,  $^{11}\text{B}$ ,  $^{13}\text{C}$ , and  $^{13}\text{N}$  [4]. As this method can not be used for the  $S_6$  space, which comprises 21 s.p. levels, the energies in this case were derived as in Ref. [10], while the pairing strengths were adjusted to reproduce the experimental gaps in  $^{12}\text{C}$  [11]. We also employ the RQRPA theoretical framework [5] with  $S_{20}$ , and  $S_{20}$  spaces. In this case, the ground state is calculated in the Relativistic Hartree-Bogoliubov model using effective Lagrangians with density dependent meson-nucleon couplings

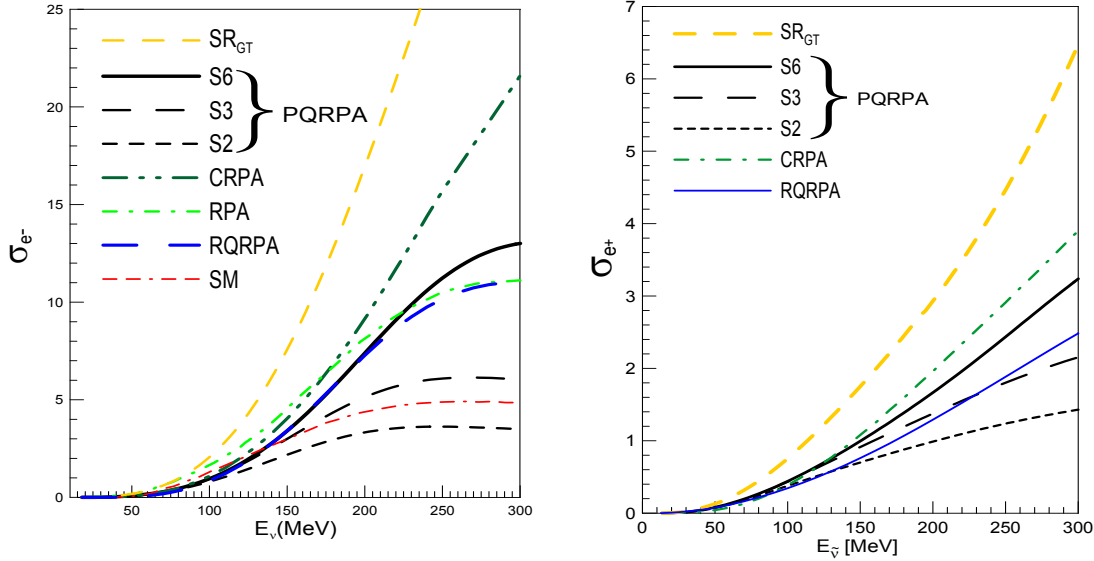


**Figure 2.** (Color online) Inclusive cross sections  $\sigma_{e^-}(E_\nu)$ , and  $\sigma_{e^+}(E_{\bar{\nu}})$  (in units of  $10^{-39}$   $\text{cm}^2$ ) for the reactions  $^{12}\text{C}(\nu_e, e^-)^{12}\text{N}$ , and  $^{12}\text{C}(\bar{\nu}_e, e^+)^{12}\text{B}$ , respectively, plotted as a function of incident neutrino and antineutrino energies. The PQRPA results within the s.p. spaces  $S_2$ ,  $S_3$ , and  $S_6$ , have the same parametrization as those on the right panel of Fig. 1. The sum rule limit  $SR_{GT}$  and several previous RPA-like calculations, namely: RPA [8], CRPA [9], and RQRPA within  $S_{20}$  for two-quasiparticle cutoff  $E_{2qp}=100$  MeV [10], as well as the shell model result [8], are also exhibited.

and DD-ME2 parameterization, and pairing correlations are described by the finite range Gogny force.

Fig. 1 shows ECS  $^{12}\text{C}_{gs}(\nu_e, e^-)^{12}\text{N}_{gs}$  plotted as a function of the incident neutrino energy  $E_\nu$  for different final energy region  $E_\nu \leq 60$  MeV (DAR region),  $E_\nu \leq 100$  MeV (supernovae neutrino signal search) and  $E_\nu \leq 250$  MeV (neutrinos oscillation search in LSND). On the left side the  $\delta$ -interaction particle-particle strength is  $t = 0$  for all  $S_N$ <sup>1</sup>, whereas on the right side  $t$  is gauged to reproduce the ground state energy of  $^{12}\text{N}$  and the  $B(GT)$  values of  $^{12}\text{N}$  and  $^{12}\text{B}$ , getting  $t = 0$  for  $S_2$  and  $S_3$ ,  $t = 0.2$  for  $S_4$ , and  $t = 0.3$  for  $S_6$ . The ECS experimental data in the DAR region are from Ref. [6].

On the left and right panels of Fig. 2 are displayed the  $^{12}\text{C}(\nu_e, e^-)^{12}\text{N}$  and  $^{12}\text{C}(\bar{\nu}_e, e^+)^{12}\text{B}$  ICS  $\sigma_{e^\mp}(E_\nu)$ , respectively. The PQRPA results within the s.p. spaces  $S_2$ ,  $S_3$  and  $S_6$ , have the same values of  $t$  as in the right panel of Fig. 1. They are compared with: i) the sum rule limit  $SR_{GT}$  obtained with an average excitation energy  $\overline{\omega_{J\pi}}$  of 17.34 MeV, ii) other RPA-like calculations, and iii) the shell model (SM).

In Fig. 3 are plotted the  $\sigma_{e^\mp}(E_\nu)$ , evaluated in RQRPA with different configuration spaces according the values of quasiparticle energy cut-off  $E_{qp}$ . One sees that the ICS increase as the configuration space increase, saturating at higher and higher energies.

Finally, Fig. 4 presents the RQRPA results for  $\sigma_{e^\mp}(E_\nu)$  with different maximal spins  $J$ . One sees that while for antineutrinos contribute spins only up to  $J = 11$ , it is needed to go up to  $J = 14$  in the case of neutrinos. It is also clear that to achieve the saturation one should go to energies larger than 600 MeV.

<sup>1</sup> This value for  $S_3$  was adopted in Ref. [4].

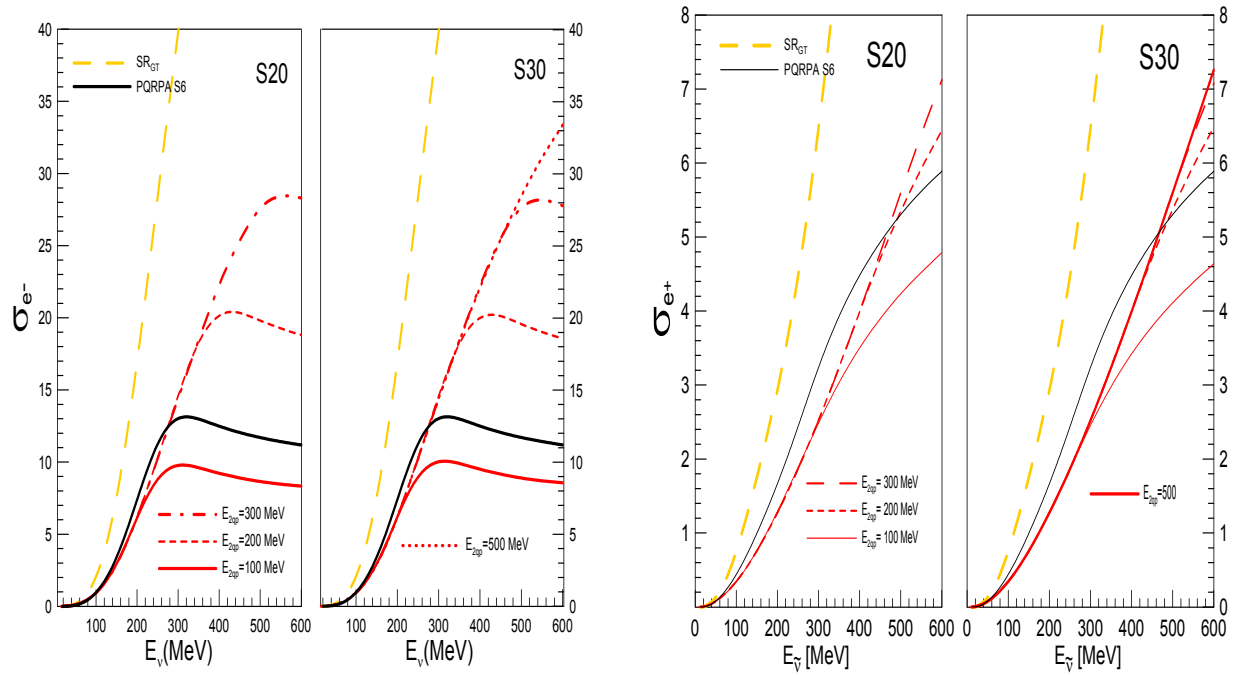


**Figure 3.** (Color online) Inclusive cross sections  $^{12}\text{C}(\nu_e, e^-)^{12}\text{N}$  (left panel) and  $^{12}\text{C}(\bar{\nu}_e, e^+)^{12}\text{B}$  (right panel) (in units of  $10^{-39} \text{ cm}^2$ ) evaluated within the RQRPA for different configuration spaces.

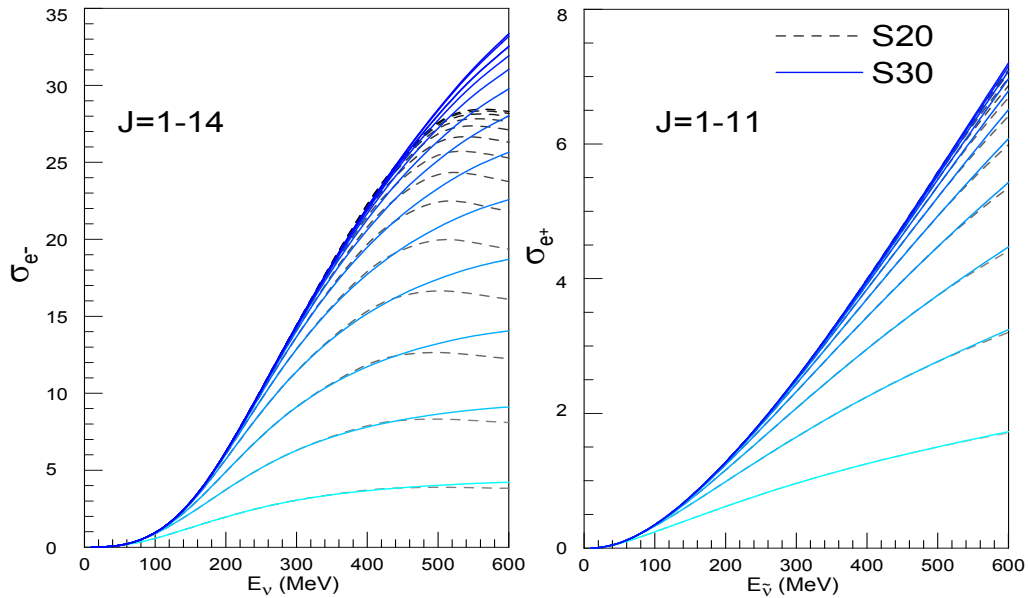


**Figure 4.** (Color online) Inclusive cross sections  $^{12}\text{C}(\nu_e, e^-)^{12}\text{N}$  (left panel) and  $^{12}\text{C}(\bar{\nu}_e, e^+)^{12}\text{B}$  (right panel) (in units of  $10^{-39} \text{ cm}^2$ ) evaluated within the RQRPA for  $E_{2qp} = 500 \text{ MeV}$  and spaces  $S_{20}$ , and  $S_{30}$ , for different maximal spins, which go up to  $J = 14$  for neutrinos, and up to  $J = 11$  for antineutrinos.

## 5. Summary

The shell model and the PQRPA are proper theoretical frameworks to describe the ground state properties of  $^{12}\text{B}$  and  $^{12}\text{N}$  and the ECS  $\sigma_{e^-}(1_1^+, E_\nu)$  for the reaction  $^{12}\text{C}(\nu_e, e^-)^{12}\text{N}$ . The ICS calculated, at difference with the exclusive ones, steadily increase, and particularly for neutrino energies larger than 200 MeV, when the size of the configuration space is augmented, in spite of including the particle-particle interaction. They approach to those of the first-forbidden sum-rule limit at low energy, but are significantly smaller at high energies both for neutrino and antineutrino. The study of the partial ICS's has been related with the proposal done in Ref. [7] of performing nuclear structure studies of forbidden processes by using low energy neutrino and antineutrino beams. We conclude that to study forbidden reactions in  $^{12}\text{C}(\bar{\nu}, e^+)^{12}\text{B}$  process, one would need  $\bar{\nu}$ -fluxes with  $E_{\bar{\nu}}$  up to  $\geq 150$  MeV, while those from Ref. [7] go up to 80 MeV only due to the feasibility of the proposed experiments.

## Acknowledgements

This work was partially supported by the Argentinean agency CONICET under contract PIP 0377, and by the U.S. DOE grants DE-FG02-08ER41533, DE-FC02-07ER41457 (UNEDF, SciDAC-2) and the Research Corporation. N. P. acknowledges support by the Unity through Knowledge Fund (UKF Grant No. 17/08), MZOS - project 1191005-1010 and Croatian National Foundation for Science.

## References

- [1] Kolbe E, Langanke K, Martínez-Pinedo G, and Vogel P, 2003 *J. Phys.* **G29**, 2569
- [2] Walecka J D 1995 *Theoretical Nuclear and Subnuclear Physics* (New York: Oxford University Press)
- [3] Krmpotić F, Mariano A, and Samana A, 2002 *Phys. Lett. B* **541** 298
- [4] Krmpotić K, Samana A, and Mariano A, 2005 *Phys. Rev. C* **71** 044319
- [5] Paar N, Nikšić T, Vretenar D, and Ring P 2004 *Phys. Rev. C* **69** 054303
- [6] Athanassopoulus C *et al.* [LSND Collaboration] 1997 *Phys. Rev. C* **55** 2078
- [7] Lazauskas R and Volpe C 2007 *Nucl. Phys. A* **792** 219
- [8] Volpe C, N. Auerbach, Colò G, Suzuki T, Van Giai N 2000 *Phys. Rev. C* **62** 015501
- [9] Kolbe E, Langanke K and Vogel P 1999 *Nucl. Phys. A* **652** 91
- [10] Paar N, Vretenar D, Marketin T and Ring P 2008 *Phys. Rev. C* **77** 024608
- [11] Samana A R, Krmpotić F, and Bertulani C A 2010 *Comp. Phys. Comm.* **181**, 1123